



Research Article

Investigation on the Temperature Distribution of Asphalt Overlay on the Existing Cement Concrete Pavement in Hot-Humid Climate in Southern China

Zuzhong Li ¹, Yayun Zhang,² Chunguang Fa,¹ Xiaoming Zou,³ Haiwei Xie,⁴ Huaxin Chen,¹ and Rui He ¹

¹School of Materials Science and Engineering, Chang'an University, Xi'an 710061, China

²Wuhan Huike Quality Testing Co., Ltd., Wuhan, Hubei 430050, China

³Liuzhou Expressway Operation Co., Ltd., Liuzhou, Guangxi 545000, China

⁴School of Traffic & Logistics Engineering, Xinjiang Agricultural University, Urumqi 830052, China

Correspondence should be addressed to Zuzhong Li; zuzhongli@126.com

Received 12 December 2019; Revised 1 December 2020; Accepted 21 January 2021; Published 10 February 2021

Academic Editor: Hui Yao

Copyright © 2021 Zuzhong Li et al. This is an open access article distributed under the Creative Commons Attribution License, which permits unrestricted use, distribution, and reproduction in any medium, provided the original work is properly cited.

Temperature is known to be one of the most important factors affecting the design and performance of asphalt concrete pavement. The distresses of asphalt overlay are closely related to its temperature, particularly in Guangxi, a hot-humid-climate region in China. This research is to analyze the impact of meteorological factors on temperature at 2 cm depth in asphalt overlay by ReliefF algorithm and also obtain the temperature prediction model using MATLAB. Two test sites were installed to monitor the temperatures at different pavement depths from 2014 to 2016; meanwhile, the meteorological data (including air temperature, solar radiation, wind speed, and relative humidity) were collected from the two meteorological stations. It has been found that the temperature at 2 cm depth experiences greater temperature variation, and the maximum and minimum temperatures of asphalt overlay, respectively, occur at 2 cm depth and on the surface. Besides, the results of ReliefF algorithm have also shown that the temperature at 2 cm depth is affected significantly by solar radiation, air temperature, wind speed, and the relative humidity. Based on these analyses, the prediction model of maximum temperature at 2 cm depth is developed using statistical regression. Moreover, the data collected in 2017 are used to validate the accuracy of the model. Compared with the existing models, the developed model was confirmed to be more effective for temperature prediction in hot-humid region. In addition, the analysis of rutting depth and overlay deformation for the two test sections with different materials is done, and the results have shown that reasonable structure and materials of asphalt overlay are vital to promote the high-temperature antideforming capability of pavement.

1. Introduction

It is well known that the strength and deformation properties of asphalt pavement strongly depend on temperature. Studies on pavement temperature, from a growing number of literatures, have been concentrated on predicting the pavement temperature profile [1–5].

In recent years, the asphalt overlays have been widely used in reconstructing old cement concrete pavement [6–8]. However, the damage in asphalt overlay, such as cracking and rutting, could be vastly induced due to the

incompatibility of the physical characteristics between asphalt concrete and cement concrete, load, and temperature. Heat transfer influences not only the deformation of old cement concrete slab but also the performance of asphalt overlay [9, 10]. Higher or lower temperature can aggravate the damage of asphalt overlays [11–13]. Especially in the hot-humid-climate regions, the rutting of asphalt overlay becomes the main distress. Therefore, an investigation on temperature distribution in asphalt overlay can contribute to selecting asphalt overlay materials and designing its structure. The relevant findings could also be helpful for the

recommendation of suitable asphalt binder performance grade.

Generally speaking, there are two main methods to determine the temperature profile of pavement, namely, analytical approach and statistical method.

Analytical approach is usually developed on the basic theory of heat transfer and meteorology method to explain thermodynamic behavior between the pavement and environment. Normally, a model or algorithm is established to predict the pavement temperature. Minhoto et al. [14] analyzed the thermal behavior of pavement using the 3D Finite Element Method (FEM) and calculated the temperature distribution of rubber asphalt pavement. Wang [15] presented an algorithm to predict one-dimensional (1D) temperature profiles in a multilayered pavement system on the basis of measured surface temperature data. Wang and Roesler [16] proposed an analytical solution to predict the one-dimensional (1D) time-dependent temperature profile in a multilayered rigid pavement system, which is modeled as a boundary value problem governed by the classic heat conduction equations and then coded by FORTRAN computer program. Aitbayev [17] analyzed the temperature distribution in asphalt concrete layers using the FEM and believed that changes of stresses and deformations in pavement and subgrade caused by temperature variation were vital to the design of pavement structure. Although all the models mentioned above can rapidly demonstrate the pavement temperature profile with less data measured in site, a large number of inputs make the approach complex and also the solution is difficult to find. The prediction of temperature profile may not be accurate enough for the continuously changing environment factors, and some parameters, such as thermal conductivity and diffusivity values of road construction materials, are uncertain because of heterogeneous characteristics, and they are also hard to be obtained.

Regression models are adopted to obtain the relationship between pavement temperature profile and environmental factors, and the statistics-based temperature profile models are built on large databases involving climatic, meteorological, geographical, and pavement geometric data. The models for analyzing the temperature field in the strategic highway research program (SHRP) and long-term pavement performance program (LTPP) are also based on the statistical method [18]. Diefenderfer et al. [19] used linear regression model to calculate the maximum and minimum pavement temperature, relying on measured data of daily ambient temperature, daily solar radiation, and depth within the pavement. Taamneh [20] developed the regression model to predict the daily maximum and minimum pavement temperature profiles from the collected data, including flexible pavement temperature and climatic data during the two years. Li et al. [21] adopted statistical regression to determine the temperature prediction model as a function of depth, average air temperature, and total solar radiation calculated in the cumulative time. Jing and Zhang [22] determined the quantitative relationships between environmental factors and pavement temperature and

established a statistical model to predict the asphalt pavement temperature in high-temperature season in Beijing. The main advantage of these statistical methods is that it gives reasonable prediction for the input data within the original sample database, but it cannot guarantee the accuracy of prediction for the other input data which may not be in the original sample database [18].

So far, considerable researches have been carried out to predict, respectively temperature profile of flexible or rigid pavement [23–26], most of which emphasized the thermodynamic behavior of pavement during the characterizing pavement temperature profile. But investigations on the temperature distribution of asphalt overlay on existing cement pavement are few [27, 28]. This pavement structure possesses the advantages of asphalt and concrete pavement, but there are still several damages for asphalt overlay, such as reflection cracking, rutting, and pothole in service. Usually, the generation of these distresses is closely related to pavement temperature. Temperature variation will play an important role in the mechanical property of asphalt overlay under special weather condition [29, 30].

Most of the models mentioned above are related to the prediction of pavement temperature in ordinary climate. The models need to be adjusted if applied for some regions with specific climate characteristics, for instance, Guangxi, in China, which is a hot-humid-climate region. Guangxi ($20^{\circ}54'$ to $26^{\circ}26'N$, $104^{\circ}29'$ to $112^{\circ}04'E$), located in southern China and connected to the South China Sea, has a humid subtropical climate. Due to the impact of marine climate, Guangxi region has lots of sunlight, rainfalls, and high humidity throughout the year. The average annual temperature is 18 to $23^{\circ}C$, while average annual precipitation is 1060 to 2658 mm and relative humidity is about 80% . Guangxi has a long and hot summer and a mild winter. Therefore, the environmental factors, such as solar radiation, air temperature, and humidity, will have a great impact on pavement temperature.

This research investigates the impact of hot-humid climate on the temperature distribution in asphalt overlay on existing cement concrete pavement by statistical regression methods. Firstly, the temperatures of asphalt overlay, existing cement concrete pavement, and existing base course were measured in the selected field test sites. Some related meteorological data, such as air temperature, solar radiation, wind speed, and relative humidity, were recorded, too. Secondly, this paper analyzed the degree of the different environmental factors influencing maximum temperature at 2 cm depth in asphalt overlay by ReliefF. Based on the measured temperature data, the multiple regression equations of maximum temperature at 2 cm depth were obtained by MATLAB software, also compared with the existing models of pavement temperature. Finally, the rutting depth and deformation of asphalt overlay for two test sections with different materials were compared.

The primary objective of this paper is to present the characteristics of the temperature distribution of asphalt overlay for hot-humid climate in Guangxi region of China

and to particularly show variation of maximum pavement temperature in hot-humid climate. This paper will contribute to material selection and structural design of asphalt overlay, which is vital for improving the high temperature stability of pavement.

2. Field Instrumentation and Data Collection

2.1. Pavement Temperature Monitoring at Project Sites

2.1.1. Field Test Sections. From over tens of locations, some parts of Guangxi region are of the most representative of hot-humid climate. This research was conducted in Nanning, Guangxi, which has an average annual precipitation of 1304.2 mm, temperature of 21.6°C, and relative humidity of 80%. Two connected pavement sections (Section I and Section II) were selected on Liunan Expressway in Guangxi (National Highway System G72), located at latitude 22°48'N and longitude 108°32'E. Meanwhile, two test sites (Site 1 and Site 2) were set up to collect the pavement temperature.

2.1.2. Pavement Structure and Testing Instrumentation. Figure 1 and Table 1 show the pavement structure and layout of temperature sensors. The asphalt overlay is 14 cm in thickness, consisting of 3.5 cm stone mastic asphalt mixtures, 8 cm dense graded asphalt mixtures, and 2.5 cm fine sand asphalt mixtures (level layer). The existing Portland cement concrete pavement is composed of 24 cm concrete pavement and 30 cm semirigid base. Between the asphalt overlay and existing Portland cement concrete pavement, there was a geotextile fabric to prevent reflective cracking from occurring in asphalt overlay.

Table 2 presents asphalt overlay structure and paving asphalt materials of the two sections. For Section II, antirut agent PR PLASTS was used in AC-25 SBS modified asphalt mixture.

Site 1 and Site 2 were instrumented with five Cu50 temperature sensors, respectively, and two data loggers to print pavement temperatures. The test range of the sensor is from -50°C to 300°C, and the accuracy is 0.1°C. Then, these sensors were placed at different depths to record the temperature profile throughout the pavement, as shown in Figure 1 and Table 1. The sensors in asphalt overlay were embedded when paving the overlay. For the existing Portland cement concrete pavements and semirigid bases, the sensors were fixed in drilled holes by using fresh cement concrete. Finally, the wires of all sensors were connected with WST-XSL Temperature Scanning Monitoring System. This system can record and print temperature data automatically with random intervals, as shown in Figure 2.

It took four years (or 1461 days) to monitor the temperature of different depth pavement from 2014 to 2017. The data collected from 2014 to 2016 at Site 1 and Site 2 were used to develop the regression models, while the data collected from 2017 at Site 2 were used to validate the models. In addition, the rutting depth of the two overlay sections was tested in 2016.

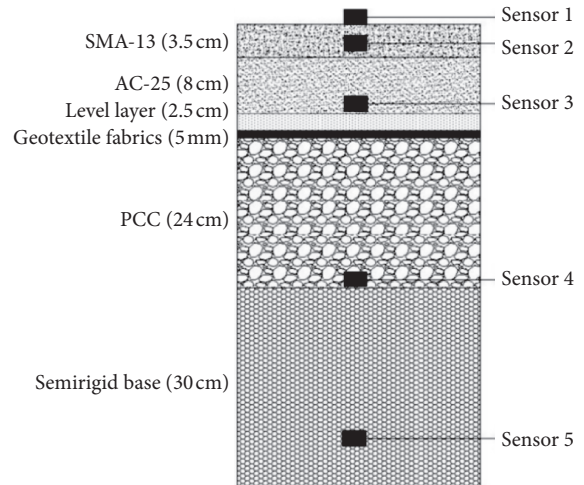


FIGURE 1: Pavement structure and layout of temperature sensors.

TABLE 1: Depths of temperature sensors in pavement.

Sensors	Sensor 1	Sensor 2	Sensor 3	Sensor 4	Sensor 5
Depth (cm)	0 (surface)	2	11.5	38.5	65

TABLE 2: Asphalt overlay structure and paving asphalt materials.

Test sections	Asphalt overlay structure	Paving asphalt materials
Section I	3.5 cm SMA-13	SBS modified asphalt
	8 cm AC-25	70# basis bitumen
	Level layer	70# basis bitumen
Section II	3.5 cm SMA-13	SBS modified asphalt
	8 cm AC-25	SBS modified asphalt
	Level layer	SBS modified asphalt



FIGURE 2: The instrument for recording and printing temperature data.

2.2. Meteorological Data Collection. In addition to the pavement temperature monitoring system, the meteorological data (including air temperature, solar radiation, wind speed, and relative humidity) were collected from the two meteorological stations at the nearby test sites, and the observation station for recording solar radiation value is shown in Figure 3. Specifically, instruments for recording air temperature and relative humidity were housed in a radiation shield to minimize the effects of solar radiation.

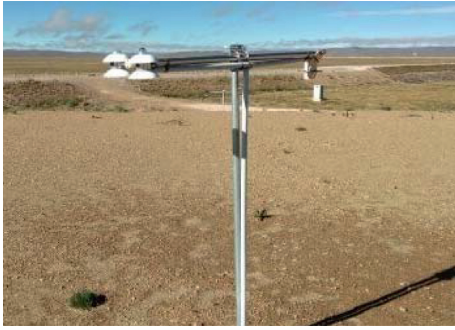


FIGURE 3: Observation station for recording solar radiation value.

3. Numerical and Regression Analysis Method

3.1. ReliefF Algorithm. The Relief algorithm is one of the most popular algorithms to feature estimation, including the first-emerging Relief algorithm for binary classification problems and the later extended ReliefF algorithm for multiple classes [31–34]. ReliefF is a feature weighting algorithm that assigns different weights to features according to the correlation of each feature and category. If the feature has different values for neighbouring instances that are of different class (termed as nearest miss), then it is awarded a higher relevance value. However, if the values of the class for the neighbouring instances are the same (termed as nearest hit), then the relevance value is decreased [35]. Therefore, the relevant features should make the samples of the same kind close and keep the samples of the heterogeneous away from each other. Due to its simple algorithm and high efficiency, ReliefF has been proved to be useful in several domains.

In this paper, the original ReliefF algorithm was used to analyze the influence of environmental factors on maximum temperature at 2 cm depth in asphalt overlay based on the collected meteorological data. The pseudocode for the ReliefF algorithm and the improved calculating flowchart are shown in the supplemental files.

3.2. Regression Analysis. Regression analysis is a set of statistical processes for estimating the relationships among variables. It involves many techniques for modeling and analyzing several variables. The `nlinfit` function is a way to implement the nonlinear regression model in MATLAB software. In this paper, the regression model was developed to relate maximum temperature at 2 cm depth in asphalt overlay to several meteorological factors, including maximum air temperature, solar radiation, wind speed, and relative humidity. To get the regression equation, the curve function was customized at first, and the format of the regression models, that is, the formula, was given. Then, the coefficients of the corresponding features were obtained by using the `nlinfit` function.

4. Characteristics of Pavement Temperature Distribution

4.1. Pavement Temperature Distribution in the Different Months. Two graphs of average monthly pavement temperature at all depths are shown in Figure 4. It is obvious that

the distribution of the pavement temperature has seasonal differences and pavement temperatures in every month show similar varying tendency. The temperature at all depths is higher in summer, especially the temperature at 2 cm depth, sometimes up to 63°C. In addition, the temperature at all depths is not too low in winter due to the mild winter in hot-humid area. Figure 4 also presents that temperature at 2 cm depth experiences the largest temperature variation all year round.

The maximum pavement temperature for several months occurs at 2 cm depth, and this results from the fact that the solar radiation at this depth is more than the heat loss caused by heat exchange. The pavement surface temperature, affected by air convection and heat reflection, is slightly lower than temperature at 2 cm depth. Besides, with the increase of pavement depth, the temperature ranges gradually decreased. In summary, the temperature at 2 cm depth, varying greatly with the season, is closely related to the distresses of asphalt overlay, such as rutting and low-temperature cracking.

4.2. Pavement Temperature Distribution in Summer. Weather Database for the Superpave Mix Design System SHRP-A-648A (Strategic Highway Research Program, 1994) has confirmed that the statistical distribution of the yearly 7-day average maximum air temperature and the yearly 1-day minimum air temperature could be used to select any particular pavement design temperature [36]. In this paper, the temperatures at all depths were measured hourly in the hottest and successive 7 days from the two test sites for three years. The typical variation of recorded pavement temperatures and air temperatures is shown in Figure 5. The data points in the graphs represent the average temperature at N h for 7 continuous days per year ($N=0, 1, 2, \dots, 23$), and then the line of the tendency was plotted according to calculating the average temperature of every three data points.

As shown in Figure 5, the temperature of asphalt overlay changes synchronously with air temperature, and the time to reach the peak temperature gradually delays with the depth. Moreover, the temperature difference between day and night at the surface is as high as 24.1°C, but the maximum temperature difference of the subgrade at 65 cm depth is only 2.4°C. It can be concluded that temperature variation is much less with the increasing depth. So the thermal stress of overlay structure mainly derives from the overlay asphalt and the existing cement concrete pavement. Besides, the maximum temperature of the pavement occurred at about 14:00 at 2 cm depth, located at the SMA layer. It is caused by high air temperatures and intense solar radiation to result in significant heat absorption of the pavement structure during the day. Due to the low thermal conductivity of asphalt mixtures, overlay prevents the heat from transferring within the pavement structure and the pavement temperature variation becomes small at night. The rising and dropping of temperature at 2 cm depth are faster than those in the other depths. The fastest increasing rate of temperature is around 10:00 and the fastest dropping rate is around 18:00 at sunset.

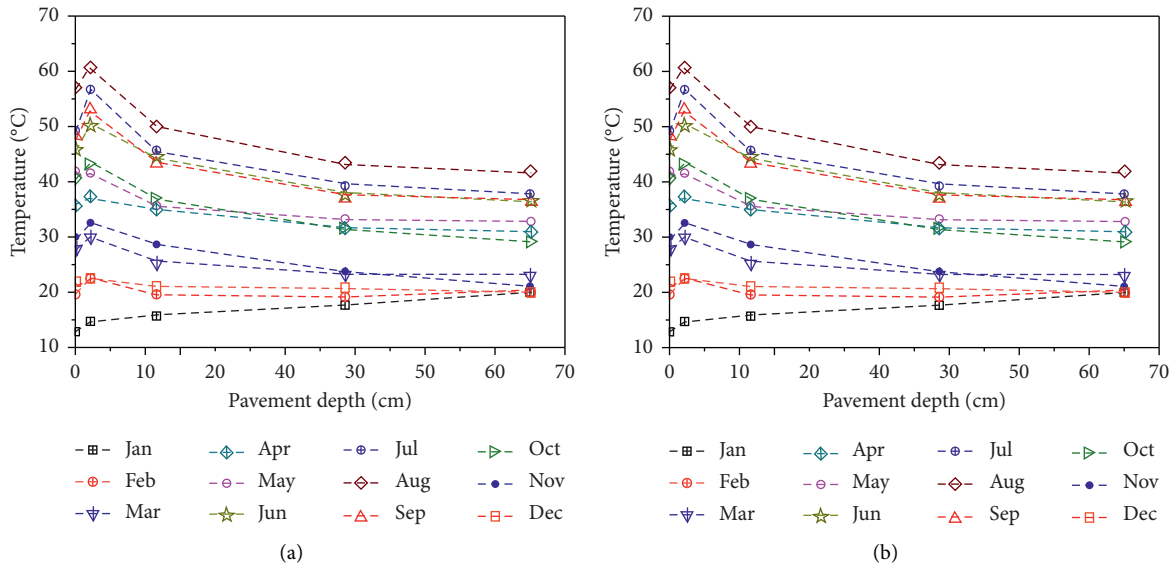


FIGURE 4: Average monthly temperature distribution of pavement: (a) Site 1. (b) Site 2.

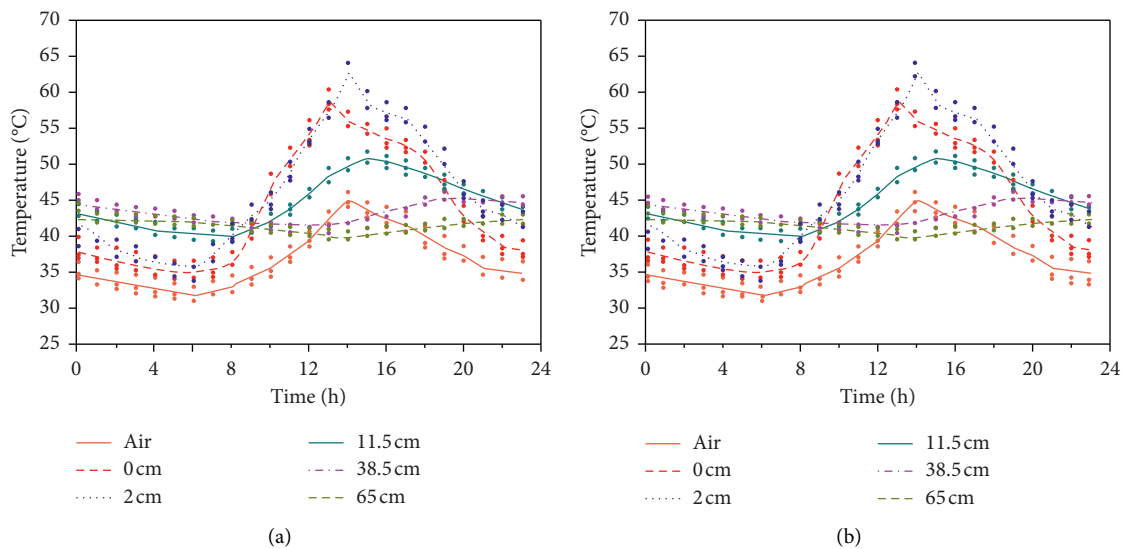


FIGURE 5: Air and pavement temperature profile over time in summer: (a) Site 1. (b) Site 2.

4.3. *Pavement Temperature Distribution in Winter.* The temperatures at all depths in winter were also measured with reference to the SHRP-A-648A. Pavement and air temperatures were measured hourly on the coldest days of every year from 2014 to 2016, and the typical variation of recorded temperatures is shown in Figure 6. There is a similar trend of temperature variation at all depths, and the asphalt layers commonly experience greater temperature variation. Generally, asphalt overlay structure temperature profile follows with the air temperature changing. Because the energy, absorbed from the solar during the day, transfers in asphalt overlay, the pavement temperatures at all depths are commonly higher than the air temperatures for the most of the time, particularly during the night. For all depths, the temperature on the surface is lower than those on other depths, affected by surface energy transmitting and air

convection in hot-humid climate. The surface layer always experiences the greatest variation in temperature for a typical day, which is about 5.6°C. In addition, the temperature gradient gradually decreases with the depth increase, and particularly the temperature is almost constant at the subgrade.

In summary, the pavement temperature roughly varies with air temperature. But the temperature ranges of all depths in summer are significantly wider than those in winter because of the hot-humid climate. The highest temperature of the pavement in summer is at 2 cm depth and the lowest temperature of the pavement in winter is on the surface. With the increase of pavement depth, the temperature tends to be stable gradually, so the temperature of subgrade is less affected by air temperature and solar radiation. Conversely, the temperature of asphalt overlay and

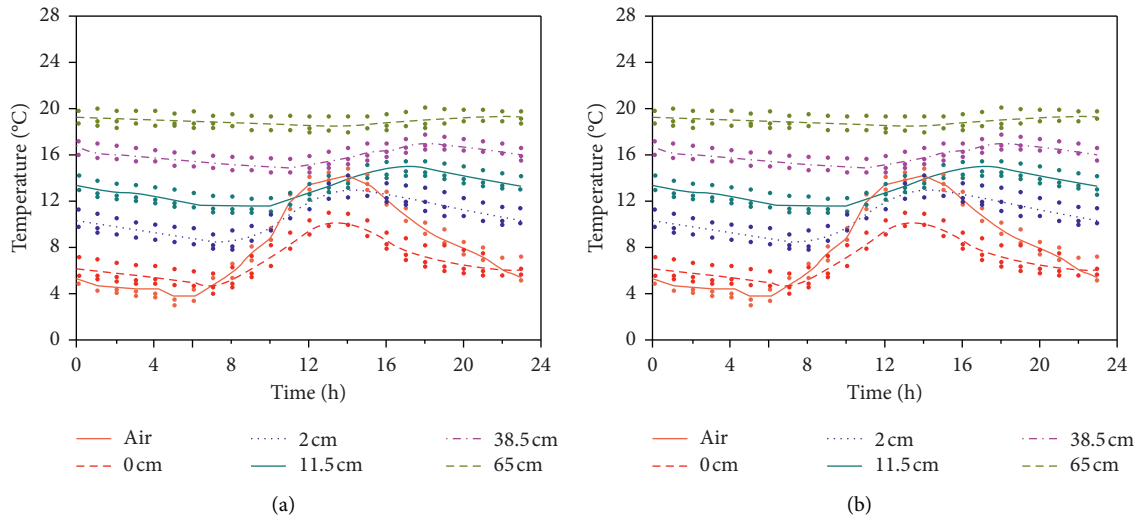


FIGURE 6: Air and pavement temperature profile over time in winter: (a) Site 1. (b) Site 2.

existing cement concrete slab are greatly affected by air temperature and solar radiation, especially the temperature at 2 cm depth [37, 38]. According to the statistical distribution of the daily maximum temperatures at 2 cm depth for three years, 4.74% of them exceeded 60°C, 22.99% of them exceeded 50°C, and 42.15% of them exceeded 40°C. Therefore, the major distresses of asphalt overlay, such as the high temperature rutting, reflective cracking, and other diseases, are closely related to temperature changes of asphalt overlay and the existing cement concrete slab.

5. Analysis of Influencing Factors and Development of Temperature Model

5.1. The Analysis of Influencing Factors on Temperature at 2 cm Depth. According to pavement temperature profile models by many researches [19, 39, 40], air temperature and solar radiation have the most significant impact on pavement temperature. A few pavement temperature profile models consider wind speed, rainfall, and relative humidity [14, 21]. According to the above pavement temperature distribution, the temperature at 2 cm depth experiences greater changes, and the maximum temperature of asphalt overlay occurs at 2 cm depth. Therefore, daily maximum air temperature, daily cumulative solar radiation, daily average wind speed, and daily average relative humidity were selected as the features of ReliefF algorithm, and then the extent of their influence on maximum temperature at 2 cm depth could be calculated. In addition, the results of ReliefF will contribute to the solution of the regression models.

The data of maximum temperature at 2 cm depth and four meteorological factors (2192 samples) were measured from the two test sites and two meteorological stations for three years. In order to facilitate the calculation, the four features were normalized, and the maximum temperature at 2 cm depth was classified into one class every 6°C at first. Then, the ReliefF algorithm was used to calculate the intra-class distance and inter-class distance of each feature.

Finally, the weight of each feature and the weight considering multifactor interaction influence were obtained, and the results are shown in Tables 3 and 4.

W_1 is the weight of daily maximum air temperature, W_2 is the weight of daily cumulative solar radiation, W_3 is the weight of daily average wind speed, and W_4 is the weight of daily average relative humidity. W_{1*2} , W_{1*3} , W_{1*4} , W_{2*3} , W_{2*4} , W_{3*4} are weights considering the interactive effect between one feature and another.

As shown in Table 3, W_2 has the greatest weight, which indicates that the daily radiation has the greatest impact on the temperature at 2 cm depth, followed by W_1 , which occupies a weight of 0.3135. So the influence of the daily maximum air temperature is also great, which is only lower than the daily radiation. On the contrary, the daily average wind speed and the daily average relative humidity have a little effect on temperature at 2 cm depth. In order to further understand the interactive effect between meteorological factors, ReliefF also gives the weights considering interactive effect between features. In Table 4, the values of W_{1*2} , W_{2*3} and W_{2*4} are relatively large, while W_{1*2} has the maximum value. It proves that the other three meteorological factors depend heavily on the daily cumulative solar radiation. The interactive effect between daily maximum air temperature and daily cumulative radiation is the strongest for temperature at 2 cm depth.

Therefore, it can be concluded that the temperature at 2 cm depth is greatly influenced by daily cumulative solar radiation and daily maximum air temperature, and the effects of daily average wind speed and daily average relative humidity were small. The temperature at 2 cm depth may strongly depend on W_1 , W_2 , W_{1*2} , W_{2*3} and W_{2*4} from the above analysis results.

5.2. Regression Analysis of Maximum Temperature at 2 cm Depth. Based on the results of ReliefF, maximum temperature at 2 cm depth can be defined as a function of daily maximum air temperature, daily cumulative solar radiation,

TABLE 3: The weight of single feature.

Feature	W_1	W_2	W_3	W_4
Weight	0.3151	0.3536	0.0409	0.0804

TABLE 4: The weight considering multifactor interaction influence.

Feature	W_{1*2}	W_{1*3}	W_{1*4}	W_{2*3}	W_{2*4}	W_{3*4}
Weight	0.3089	0.0711	0.1921	0.2342	0.2720	0.0001

daily average wind speed, and daily average relative humidity. The temperature prediction model in form of linear regression model is expressed as follows:

$$T_{2.0\max} = a_1 + a_2 \cdot T_{\max} + a_3 \cdot L_{\text{total}} + a_4 \cdot V_{\text{ave}} + a_5 \cdot R_{\text{ave}}, \quad (1)$$

where $T_{2.0\max}$ = maximum temperature at 2 cm depth ($^{\circ}\text{C}$); T_{\max} = daily maximum air temperature ($^{\circ}\text{C}$); L_{total} = daily cumulative solar radiation (MJ/m^2); V_{ave} = daily average wind speed (m/s); R_{ave} = daily average relative humidity (%); and a_i ($i = 1, 2, \dots, 5$) are regression coefficients.

$$T_{2.0\max} = b_1 T_{\max}^2 + b_2 L_{\text{total}}^2 + b_3 V_{\text{ave}}^2 + b_4 R_{\text{ave}}^2 + b_5 T_{\max} L_{\text{total}} + b_6 T_{\max} V_{\text{ave}} + b_7 T_{\max} R_{\text{ave}} + b_8 L_{\text{total}} V_{\text{ave}} + b_9 L_{\text{total}} R_{\text{ave}} + b_{10} V_{\text{ave}} R_{\text{ave}} + b_{11} T_{\max} + b_{12} L_{\text{total}} + b_{13} V_{\text{ave}} + b_{14} R_{\text{ave}} + b_{15}, \quad (3)$$

where b_i ($i = 1, 2, \dots, 15$) are regression coefficients.

Similarly, all coefficients for equation (3) were obtained by MATLAB on the basis of maximum temperature at 2 cm

$$T_{2.0\max} = 0.0304T_{\max}^2 - 0.0700L_{\text{total}}^2 - 0.2617V_{\text{ave}}^2 + 12.9800R_{\text{ave}}^2 + 0.0183T_{\max}L_{\text{total}} - 0.2504T_{\max}V_{\text{ave}} + 4.3458T_{\max}R_{\text{ave}} + 0.6838L_{\text{total}}V_{\text{ave}} - 4.9264L_{\text{total}}R_{\text{ave}} + 11.5512V_{\text{ave}}R_{\text{ave}} - 4.1823T_{\max} + 5.6518L_{\text{total}} - 11.6655V_{\text{ave}} - 121.5986R_{\text{ave}} + 104.4172. \quad (4)$$

The evaluation of the temperature model (equation (4)) versus the measured maximum temperature at 2 cm depth is presented in Figure 8. Results from the model overlap the 45-degree line, indicating a very good fit. It can be seen that the improved model is more effective than linear regression model, especially when pavement temperature exceeds 35°C . R^2 is 0.9842 and the standard deviation is 1.32. It is clear that the standard deviation of equation (4) decreased by 8.33% compared to equation (3), so equation (4) shows higher accuracy.

5.3. Validation and Application of the Improved Pavement Temperature Model. The improved model (equation (4)) for predicting maximum temperature at 2 cm depth was validated by the measured data collected in 2017 at Site 2. Firstly, based on the collected meteorological data in 2017, the

The input data (2192 samples) were derived from the two test sites and two weather stations for three years. The nlinfit function in MATLAB was used to calculate all coefficients in equation (1), so the model can be determined as follows:

$$T_{2.0\max} = -1.2251 + 0.4098T_{\max} + 2.4909L_{\text{total}} - 1.4286V_{\text{ave}} - 1.7946R_{\text{ave}}. \quad (2)$$

In addition, the pavement temperature prediction (equation (2)) was plotted against measured temperatures, as shown in Figure 7. R^2 and standard deviation are 0.9814 and 1.44, respectively.

Furthermore, considering that the interaction between features also has a relatively high effect on the temperature at 2 cm depth, the new temperature prediction model was developed in the form of nonlinear regression model; and the improved model can be described as follows:

depth and meteorological data, and the improved model is given:

maximum temperature at 2 cm depth was predicted by the improved model. Then, the model validation was performed by comparing the measured and predicted maximum temperatures at 2 cm depth in Figure 9. It is obvious that results from the improved model overlap the 45-degree line, indicating a very good fit. R^2 is 0.9693 and the standard deviation is 1.28. Meanwhile, the effectiveness of the improved model for maximum temperature at 2 cm depth in Guangxi region has been validated.

For other regions with hot-humid climate, the improved model (equation (4)) still has some applicability. Through the collection of meteorological data, the maximum pavement temperature at 2 cm depth can be calculated every day by equation (4). The range and distribution of the maximum pavement temperature at 2 cm depth are very important for the material selection and structure design of asphalt pavement or overlay. The

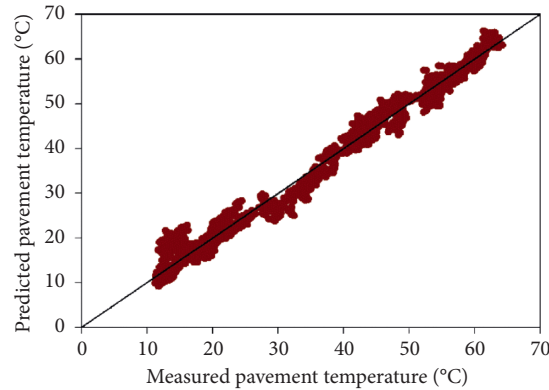


FIGURE 7: Measured versus predicted maximum temperature at 2 cm depth [equation (2)] during 2014–2016.

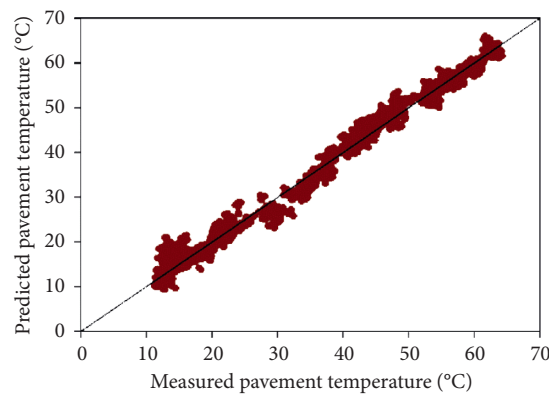


FIGURE 8: Measured versus predicted maximum temperature at 2 cm depth [equation (4)] during 2014–2016.

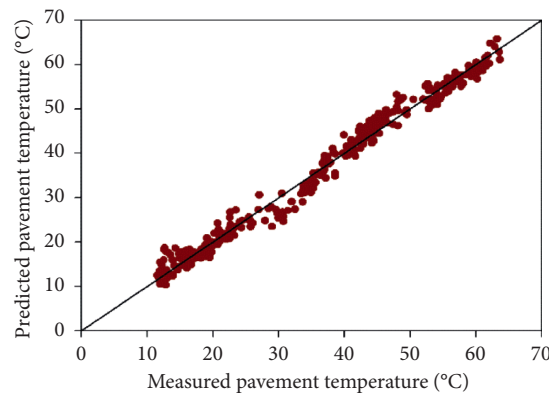


FIGURE 9: Measured versus predicted maximum temperature at 2 cm depth in 2017.

longer high temperature lasts, the more stable pavement materials or structure will be chosen as far as possible.

5.4. Comparison with Other Existing Models. The prediction models developed by Taamneh [20] (termed as Model 1) and Ariawan et al. [41] (termed as Model 2) are compared with the improved model in this work in Figure 10. The former two models are regression models developed from measured pavement temperature and meteorological data. The two models are discussed as follows.

Based on the meteorological data from the meteorological station in this work, the maximum temperature at 2 cm depth was calculated by applying these models. Then, the predicted temperatures were subtracted from the measured temperatures to produce a set of residuals, and the cumulative frequencies of the absolute residuals are shown in Figure 10. It can be seen that 90% of the absolute residuals of the improved model are within 3.5, which proves higher accuracy of the improved model in this research. On the contrary, for Model 1 and Model 2, the cumulative frequencies of residual values within 8 are 56%

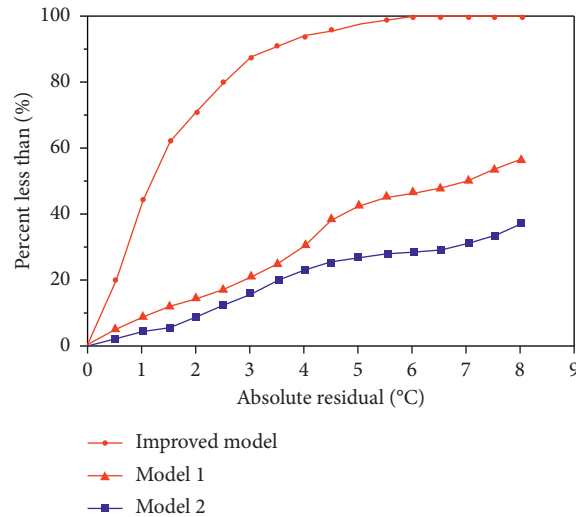


FIGURE 10: Comparisons of prediction errors between Model 1, Model 2, and the improved model.

and 37%, respectively. It is not so effective for Model 1 and Model 2 to predict the maximum temperature at 2 cm depth in hot-humid areas. But, in general, Model 1 is better than Model 2.

Possible reasons for this result were discussed. The meteorological data and pavement temperature used to develop Model 1 were collected from a continental climate zone, Ohio, USA. It will be hot in summer and cold with less rain in winter. The meteorological data used to establish the regression model do not present the characteristics of a hot-humid climate. Although Model 1 took into account environmental factors including humidity and solar radiation, it was still not suitable for typical hot-humid regions. On the contrary, the data used to develop Model 2 were collected from a tropical and humid region, Indonesia, but it neglected the important influence of solar radiation on pavement temperature. According to the analysis of factors that influences pavement temperature in this research, the daily cumulative radiation has the most significant impact on the temperature at 2 cm depth. Meanwhile, these two models were linear regression models, and the interaction of influencing factors was not considered when the models were established.

6. Analysis of Rutting Depth and Damage

6.1. Rutting Depth. For Section I and Section II, the mixtures of the following layer and level layer in Section I were produced with 70# basis bitumen, while the mixtures of the following layer mixed with antirut agent PR PLASTS and level layer in Section II were produced with SBS modified asphalt. Paved after three years, the rutting depths of two sections were measured, as shown in Figure 11.

Figure 11(a) presents the distribution of rutting depth in Section I, the majority of which is between 10 mm and 20 mm. However, the depth over 20 mm accounted for about 16.9%, and the maximum depth was up to about 50 mm, occurring near its top of large longitudinal slope. So rutting had become a primary disease in Section I and maintenance

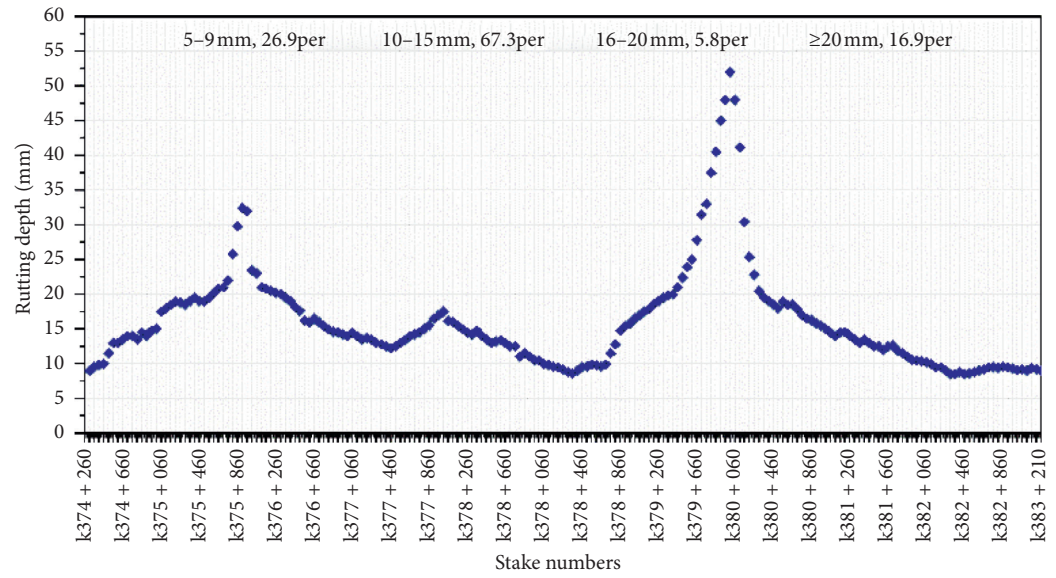
for rutting had been carried out. For general rutting, high viscoelastic emulsified asphalt microsurfacing was used for maintenance, while for severe rutting on uphill section (rutting depth is close to 50 mm), it was usually milled and then repaved according to structure of Section 2.

In contrast, Figure 11(b) displays the distribution of rutting depth in Section II, the most part of which is between 5 mm and 15 mm. Although there was a fraction of rutting depth over 20 mm, it accounts for small percentage of the total, only 3.8%. At present, the large-scale maintenance for Section II is not required. Therefore, the bonding material has an important effect on the rutting resistance of asphalt overlay. Particularly, in hot-humid climate, priority should be given to modified asphalt and antirut agent for overlay in order to improve high temperature stability of asphalt mixture.

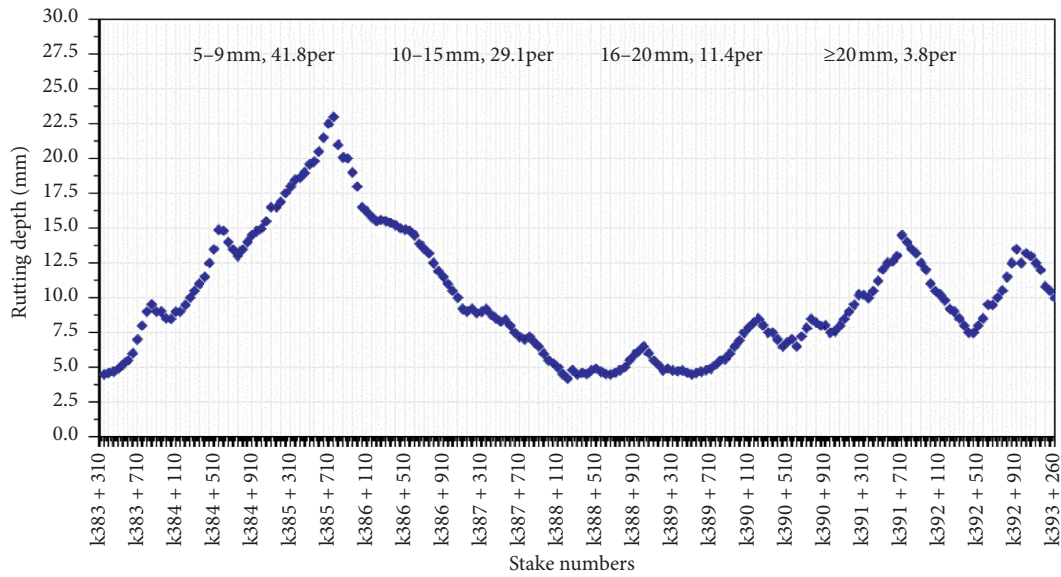
6.2. Damage Analysis. For the most serious rutting damage from Section I, at one month and the third year since it was paved, core sample of asphalt overlay was drilled out, as shown in Figure 12. The thickness of the following layer changed from 8 cm to 4.5 cm. Aggregate in it could be moved and the skeletons of mixture could be transformed. Besides, the slippage of level layer occurred entirely because its interlaminar shear strength is too weak. So, the deficiency of high temperature stability for the following layer and level layer is the dominant factor that aggravates the rutting formation and development.

On the basis of the former statistical analysis of the daily maximum temperature at 2 cm depth for three years, the proportion over 40°C accounts for 42.15%. In hot-humid climate, the higher temperature remains longer to aggravate rutting damage.

Although the temperature of asphalt overlay at 2 cm depth reached the highest value, heat in asphalt overlay transferred from 2 cm depth to leveling layer, the section of which was affected by high temperature, and led to rutting deformation.



(a)



(b)

FIGURE 11: The rutting depth of two sections after three years: (a) Section I. (b) Section II.



FIGURE 12: Core sample test of asphalt overlay: (a) after one month; (b) after three years.

7. Conclusions

A research was undertaken to characterize the temperature distribution of asphalt overlay on the existing cement concrete pavement in Guangxi region, which has a hot-humid climate. It is found that the temperature at 2 cm depth in asphalt overlay experienced greater temperature variation. With the increase of pavement depth, the impact of air temperature and solar radiation on pavement temperature gradually weakened. The coverage of the asphalt layer can significantly reduce the thermal stress of the old cement concrete slab.

An effective temperature prediction model was developed to calculate maximum temperature at 2 cm depth in asphalt overlay. This regression model focused on four main factors: daily maximum air temperature, daily cumulative solar radiation, daily average wind speed, and daily average relative humidity. Among them, solar radiation is found to have greatest impact on pavement temperature, followed by air temperature. Through data fitting, the predicted temperatures at 2 cm depth are in good agreement with the measured values. Compared with other existing models, the developed model has better applicability for pavement temperature prediction in hot-humid regions.

The rutting depth of Section I is obviously greater than that of Section II, so it can be concluded that modified asphalt must be used as bonding material for asphalt overlay in hot-humid regions; meanwhile, the antirrut agent must be added. The deformation in core sample of Section I also indicates that it is not feasible to use basis bitumen as the bonding material in asphalt overlay. The strength and deformation properties of asphalt concrete pavement are strongly influenced by its temperature, and the analysis of environmental impact factors and temperature prediction models in this research can be used with reference to material selection and structural design of asphalt overlay.

Data Availability

The pavement temperature distribution data used to support the findings of this study are included within the article, the pseudocode for the ReliefF algorithm and calculating flowchart are included within the supplementary information file, and other relevant data are available from the corresponding author upon request.

Additional Points

Highlights. (i) The characteristics of temperature distribution of asphalt overlay in hot-humid climate in Guangxi Zhuang Autonomous Region of China were presented. (ii) The temperature at 2 cm depth in asphalt overlay is affected significantly by solar radiation, followed by air temperature. (iii) An effective temperature prediction model for asphalt overlay was developed using statistical method. (iv) Priority should be given to modified asphalt and antirrut agent for asphalt overlay in hot-humid regions.

Conflicts of Interest

The authors declare that they have no conflicts of interest.

Acknowledgments

The authors were funded by the Natural Science Foundation of Xinjiang Uygur Autonomous Region (Science & Technology Department of Xinjiang Uygur Autonomous Region, no. 2019D01A44), the Transportation Science and Technology Project of Guangxi (Department of Transport of Guangxi Zhuang Autonomous Region, no. 201310031), the National Natural Science Foundation of China (Natural Science Funds Commission, no. 51508030), Fundamental Research Funds for the Central Universities of China (Ministry of Education of the People's Republic of China, nos. 300102318401, 300102318501, and 310831172201), and the Special Fund for Basic Scientific Research of Central Colleges, Chang'an University (Ministry of Education of the People's Republic of China, no. 3001102319501).

Supplementary Materials

The pseudocode for the ReliefF algorithm and the improved calculating flowchart are shown in the supplemental files. (*Supplementary Materials*)

References

- [1] A. K. Schindler, J. M. Ruiz, R. O. Rasmussen, G. K. Chang, and L. G. Wathne, "Concrete pavement temperature prediction and case studies with the FHWA HIPERPAV models," *Cement and Concrete Composites*, vol. 26, no. 5, pp. 463–471, 2004.
- [2] S.-M. Kim and J. H. Nam, "Measurements and experimental analysis of temperature variations in Portland cement concrete pavement systems," *Road Materials and Pavement Design*, vol. 11, no. 3, pp. 745–771, 2010.
- [3] C. Liu and D. Yuan, "Temperature distribution in layered road structures," *Journal of Transportation Engineering*, vol. 126, no. 1, pp. 93–95, 2000.
- [4] Y. Liu, Z. Qian, and H. Hu, "Thermal field characteristic analysis of steel bridge deck during high-temperature asphalt pavement paving," *KSCE Journal of Civil Engineering*, vol. 20, no. 7, pp. 2811–2821, 2016.
- [5] Y. Qin and J. E. Hiller, "Modeling the temperature and stress distributions in rigid pavements: impact of solar radiation absorption and heat history development," *KSCE Journal of Civil Engineering*, vol. 15, no. 8, pp. 1361–1371, 2011.
- [6] A. Bae, D. Lee, and J. Y. Tan, "Smoothness improvement by HMA overlay on very rough surface in urban tunnel expressway," *KSCE Journal of Civil Engineering*, vol. 21, no. 6, pp. 2177–2185, 2017.
- [7] J. Mikolaj, L. Remek, and M. Macula, "Asphalt concrete overlay optimization based on pavement performance models," *Advances in Materials Science and Engineering*, vol. 2017, Article ID 6063508, 10 pages, 2017.
- [8] Y. Zhong and H. Liu, "Theoretical analysis of overlay resisting crack propagation in old cement concrete pavement," *Road Materials and Pavement Design*, vol. 15, no. 3, pp. 701–711, 2014.

- [9] N. P. Sharifi and K. C. Mahboub, "Application of a PCM-rich concrete overlay to control thermal induced curling stresses in concrete pavements," *Construction and Building Materials*, vol. 183, pp. 502–512, 2018.
- [10] Z. Sun, Y. Xu, Y. Tan, L. Zhang, H. Xu, and A. Meng, "Investigation of sand mixture interlayer reducing the thermal constraint strain in asphalt concrete overlay," *Construction and Building Materials*, vol. 171, pp. 357–366, 2018.
- [11] S. Li, X. Liu, and Z. Liu, "Interlaminar shear fatigue and damage characteristics of asphalt layer for asphalt overlay on rigid pavement," *Construction and Building Materials*, vol. 68, pp. 341–347, 2014.
- [12] S. Erlingsson, "Rutting development in a flexible pavement structure," *Road Materials and Pavement Design*, vol. 23, no. 13, pp. 218–234, 2012.
- [13] X. Zhao, A. Shen, and B. Ma, "Temperature adaptability of asphalt pavement to high temperatures and significant temperature differences," *Advances in Materials Science and Engineering*, vol. 2018, Article ID 9436321, 16 pages, 2018.
- [14] M. C. Minhoto, J. Pais, and P. A. Pereira, "Asphalt pavement temperature prediction," *Road Materials and Pavement Design*, vol. 2006, pp. 193–207, 2006.
- [15] D. Wang, "Analytical approach to predict temperature profile in a multilayered pavement system based on measured surface temperature data," *Journal of Transportation Engineering*, vol. 138, no. 5, pp. 674–679, 2012.
- [16] D. Wang and J. R. Roesler, "One-dimensional temperature profile prediction in multi-layered rigid pavement systems using a separation of variables method," *International Journal of Pavement Engineering*, vol. 15, no. 5, pp. 373–382, 2012.
- [17] B. K. Aitbayev, "Modeling of temperature field in flexible pavement," *Indian Geotechnical Journal*, vol. 45, no. 4, pp. 371–377, 2015.
- [18] D. Wang, "Simplified analytical approach to predicting asphalt pavement temperature," *Journal of Materials in Civil Engineering*, vol. 27, no. 12, 2015.
- [19] B. K. Diefenderfer, I. L. Al-Qadi, and S. D. Diefenderfer, "Model to predict pavement temperature profile: development and validation," *Journal of Transportation Engineering*, vol. 132, no. 2, pp. 162–167, 2006.
- [20] M. Taamneh, "Temperature profile prediction for flexible pavement structures," *HKIE Transactions*, vol. 23, no. 3, pp. 150–156, 2016.
- [21] Y. Li, L. Liu, and L. Sun, "Temperature predictions for asphalt pavement with thick asphalt layer," *Construction and Building Materials*, vol. 160, pp. 802–809, 2018.
- [22] C. Jing and J. X. Zhang, "Prediction model for asphalt pavement temperature in high-temperature season in Beijing," *Advances in Civil Engineering*, vol. 2018, Article ID 1837952, 11 pages, 2018.
- [23] J. Chen, H. Wang, and H. Zhu, "Analytical approach for evaluating temperature field of thermal modified asphalt pavement and urban heat island effect," *Applied Thermal Engineering*, vol. 113, pp. 739–748, 2017.
- [24] K. Huang, D. G. Zollinger, X. Shi, and P. Sun, "A developed method of analyzing temperature and moisture profiles in rigid pavement slabs," *Construction and Building Materials*, vol. 151, pp. 782–788, 2017.
- [25] Y. X. Zheng, Y. C. Cai, and Y. M. Zhang, "Study on temperature field of asphalt concrete pavement," in *Proceedings of the GeoHunan International Conference 2011*, Hunan, China, 2011.
- [26] Y. Qin and J. E. Hiller, "Modeling temperature distribution in rigid pavement slabs: impact of air temperature," *Construction and Building Materials*, vol. 25, no. 9, pp. 3753–3761, 2011.
- [27] P. Yang, N. X. Han, W. J. Long, T. Y. Zeng, and J. M. Mai, "Study on temperature field distribution of asphalt overlay on existing cement pavement," *Advances in Engineering Research (AER)*, vol. 143, pp. 196–203, 2017.
- [28] M. J. C. Minhoto, J. C. Pais, P. A. A. Pereira, and L. G. Picado-Santos, "The influence of temperature variation in the prediction of the pavement overlay life," *Road Materials and Pavement Design*, vol. 6, no. 3, pp. 365–384, 2011.
- [29] F. Schlosser, J. Mikolaj, V. Zatkalikova, J. Sramek, D. Durekova, and L. Remek, "Deformation properties and fatigue of bituminous mixtures," *Advances in Materials Science and Engineering*, vol. 2013, Article ID 701764, 7 pages, 2013.
- [30] S. Kumlai, P. Jitsangiam, and P. Pichayapan, "The implications of increasing temperature due to climate change for asphalt concrete performance and pavement design," *KSCCE Journal of Civil Engineering*, vol. 21, no. 4, pp. 1222–1234, 2017.
- [31] K. Kira and L. A. Rendell, "A practical approach to feature selection," in *Proceedings of the 9th International Workshop on Machine Learning*, San Francisco, CA, USA, 1992.
- [32] I. Kononenko, "Estimating attributes: analysis and extensions of relief," in *Proceedings of the 1994 European Conference on Machine Learning*, Catania, Italy, 1994.
- [33] O. Reyes, C. Morell, and S. Ventura, "Scalable extensions of the ReliefF algorithm for weighting and selecting features on the multi-label learning context," *Neurocomputing*, vol. 161, pp. 168–182, 2015.
- [34] M. Robnik-Sikonja and I. Kononenko, "Theoretical and empirical analysis of ReliefF and RReliefF," *Machine Learning*, vol. 53, pp. 23–69, 2003.
- [35] I. Slavkov, J. Karcheska, D. Kocev, and S. Dzeroski, "HMC-ReliefF: feature ranking for hierarchical multi-label classification," *Computer Science and Information Systems*, vol. 15, no. 1, pp. 187–209, 2017.
- [36] G. A. Huber, *Weather Database for the SUPERPAVE Mix Design System, Strategic Highway Research Program*, National Research Council, Washington, DC, USA, 1994.
- [37] Q. Zhang, "Study on temperature field of cement concrete pavement and analysis of meteorological factors in Beijing area," *Highway*, vol. 7, pp. 44–48, 2011, in Chinese.
- [38] W. S. Xu, T. Wei, and H. Luo, "Analysis of thermal stress response in asphalt overlay," in *Proceedings of the 9th International Conference of Chinese Transportation Professionals (ICCTP)*, Harbin, China, 2009.
- [39] Å. Hermansson, "Mathematical model for calculation of pavement temperatures: comparison of calculated and measured temperatures," *Transportation Research Record: Journal of the Transportation Research Board*, vol. 1764, no. 1, pp. 180–188, 2001.
- [40] M. J. C. Minhoto, J. C. Pais, and P. Pereira, "Prediction of asphalt pavement temperature using 3-D finite element method," in *Proceedings of the Transportation Research Board 84th Annual Meeting*, Washington, DC, USA, 2005.
- [41] I. M. A. Ariawan, B. S. Subagio, and B. H. Setiadjai, "Development of asphalt pavement temperature model for tropical climate conditions in West Bali region," *Procedia Engineering*, vol. 125, pp. 474–480, 2015.